

ESSA RESEARCH LABORATORIES  
National Severe Storms Laboratory  
Norman, Oklahoma  
June 1968

Thunderstorm-Environment Interactions  
Revealed by Chaff Trajectories  
in the Mid-Troposphere

56.4442

I 87

02343



Technical Memorandum ERLTM-NSSL 39

U.S. DEPARTMENT OF COMMERCE / ENVIRONMENTAL SCIENCE SERVICES ADMINISTRATION

U.S. DEPARTMENT OF COMMERCE  
ENVIRONMENTAL SCIENCE SERVICES ADMINISTRATION  
RESEARCH LABORATORIES

ESSA Research Laboratories Technical Memorandum-NSSL 39

THUNDERSTORM-ENVIRONMENT INTERACTIONS REVEALED BY  
CHAFF TRAJECTORIES IN THE MID-TROPOSPHERE

James C. Fankhauser  
National Center for Atmospheric Research  
Boulder, Colorado 80302

NATIONAL SEVERE STORMS LABORATORY  
TECHNICAL MEMORANDUM NO. 39

NORMAN, OKLAHOMA 73069  
JUNE 1968





ENVIRONMENTAL SCIENCE SERVICES ADMINISTRATION

RESEARCH LABORATORIES

NATIONAL SEVERE STORMS LABORATORY TECHNICAL MEMORANDA

The National Severe Storms Laboratory, Norman, Oklahoma, in cooperation with other government groups, and with units of commerce and education, seeks to increase understanding of severe local storms, to improve methods for detecting these storms and for measuring associated meteorological parameters, and to promote the development and applications of weather radar.

Reports by the cooperating groups are printed as NSSL Technical Memoranda, a sub-series of the ESSA Technical Memorandum series, to facilitate prompt communication of information to vitally interested parties and to elicit their constructive comments. These Memoranda are not formal scientific publications.

The NSSL Technical Memoranda, beginning with No. 28, continue the sequence established by the U.S. Weather Bureau National Severe Storms Project, Kansas City, Missouri. Numbers 1-22 were designated NSSP Reports. Numbers 23-27 were NSSL Reports, and 24-27 appeared as a subseries of Weather Bureau Technical Notes.

Reports in this series are available from the Clearinghouse for Federal Scientific and Technical Information, U.S. Department of Commerce, Sills Bldg., Port Royal Road, Springfield, Virginia 22151.

## ABSTRACT

Some physical convective storm models suggest that large thunderstorms create effective barriers to the environmental airflow through the process of vertical momentum transport in their vigorous updrafts and downdrafts. Hydrodynamically, the relative air motion near a thunderstorm has been considered analogous to potential flow around a solid cylinder. Appraisals of thunderstorm water and energy budgets demonstrate, on the other hand, that potentially cold dry air must enter the storm circulation at some midcloud level aloft, in order to supply air with properties observed in the downdraft region beneath the storm.

Both of these opposed conditions are supported by analysis of the trajectories of chaff deposited at midcloud level on the upwind and downwind sides of a mature thunderstorm. Individual chaff targets, initially located on the upwind flanks of the storm, deviate around and accelerate relative to the radar precipitation echo; however, a chaff target released immediately upstream eventually becomes absorbed by the storm echo.

Circulations derived from the chaff motion are compared with independent wind measurements obtained from an airborne Doppler system and rawinsondes, and to flow characteristics demonstrated by classical hydrodynamical experiments.

## TABLE OF CONTENTS

	Page
ABSTRACT	iv
1. INTRODUCTION	1
2. STORM EVOLUTION AND ATTENDING ATMOSPHERIC CONDITIONS	1
3. EXPERIMENTAL AND ANALYTICAL PROCEDURES	5
4. DISCUSSION OF RELATIVE AIRFLOW	8
5. SUMMARY AND CONCLUSIONS	12
6. ACKNOWLEDGMENTS	13
7. REFERENCES	13

# THUNDERSTORM-ENVIRONMENT INTERACTIONS REVEALED BY CHAFF TRAJECTORIES IN THE MID-TROPOSPHERE

James C. Fankhauser

## 1. INTRODUCTION

A vital tenet in the development of the dynamical thunderstorm model presented by Newton and Newton (1959) is that vigorous vertical drafts within large cumulonimbus clouds enable persistent storms to behave as effective barriers to the environmental airflow. The model proposes that resistance to shearing tendencies aloft is provided by vertical transport of conserved horizontal momentum in rising or falling air parcels. Numerous recent endeavors to explain anomalous thunderstorm motion (Fujita, 1965; Goldman, 1966; Harrold, 1966; Fujita and Grandoso, 1966; Fankhauser, 1967) have followed Byers' (1942) suggestion that the relationship of a thunderstorm's circulation to the current in which it is embedded may be analogous to hydrodynamic theory pertaining to the behavior of rotating solid cylinders in potential stream flow.

Normand's (1946) important recognition that potentially cool air descending in downdrafts must, according to its conserved properties, enter the cloud circulation at some level aloft stands in contrast to the concept of a totally rigid cloud column. His premise is substantiated by Brownings's (1964) analysis of airflow near and within severe thunderstorms and by Newton's (1966) convective storm mass and water budget assessments.

Comprehensive data collected in Oklahoma by the National Severe Storms Laboratory on May 28, 1967, provide a basis for examining each of the above hypotheses. A definition of the airflow around an isolated thunderstorm is obtained from the motion of chaff targets, which were systematically released from an aircraft near the 500-mb level on the upwind and downwind sides of the storm. Chaff and precipitation echoes were monitored by RHI and PPI radars operating in L, S, C, and X band ranges.

Circulations derived from chaff winds are compared with kinematical and thermodynamical properties based on data provided by a mesonetwork or rawinsondes and an airborne Doppler navigational system. Similarities between the observed flow and that demonstrated by classical hydrodynamical experiments are also discussed.

## 2. STORM EVOLUTION AND ATTENDING ATMOSPHERIC CONDITIONS

The dynamic and thermodynamic characteristics of the atmosphere over Oklahoma early on May 28, 1967, were only marginally conducive to thunderstorm formation. Stability indexes on morning soundings were slightly negative, and, at the synoptic scale, differential advection indicated little chance for significant destabilization.

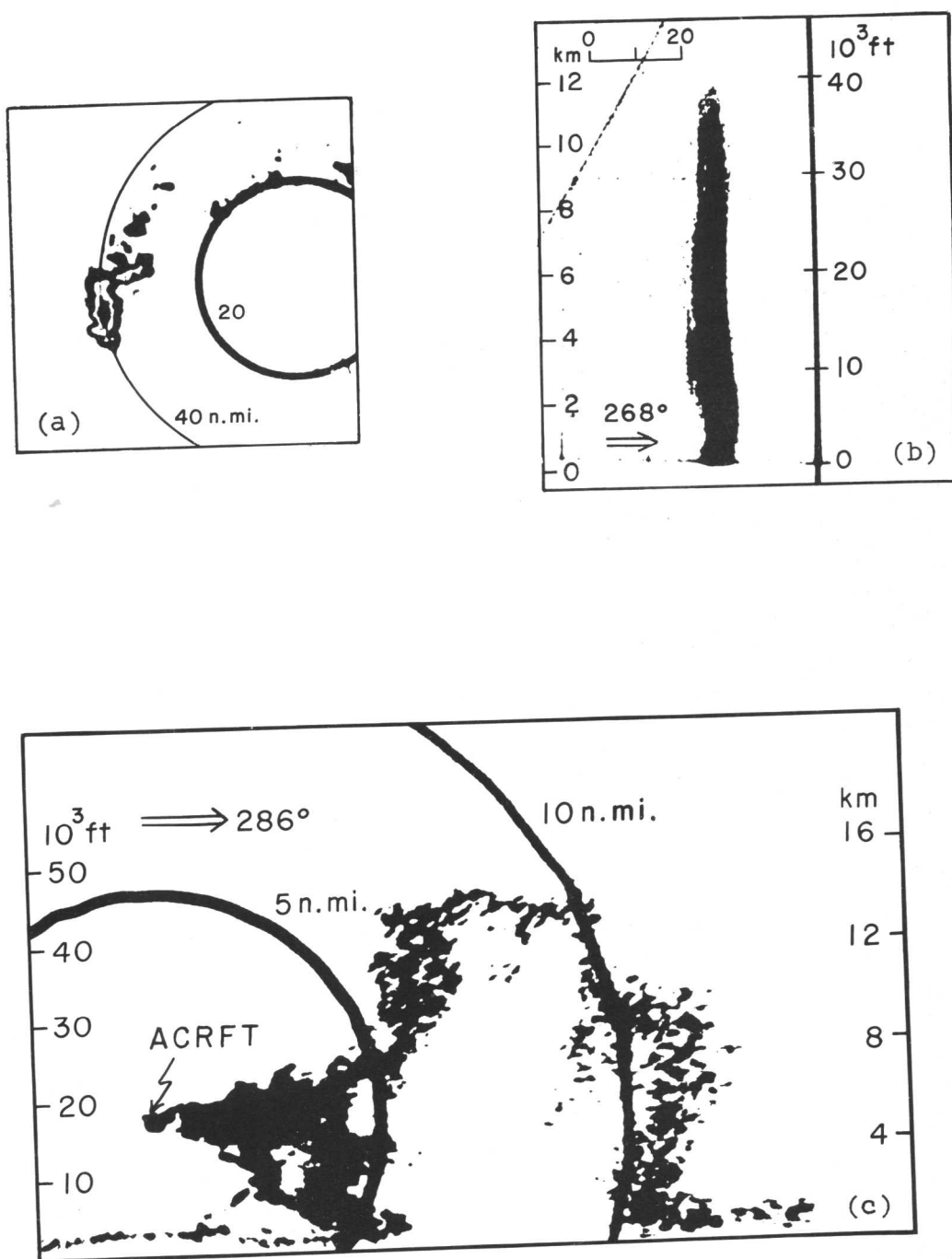


Figure 1. Radar echo configurations, May 28, 1967. (a) NSSL, WSR-57, PPI at 1545 CST. Intensity contours at 10-dB intervals. (b) NSSL, MPS-4, RHI at 1544 CST. (c) RFF, RDR-1D, RHI at 1548 CST; echo cancellation at 16-dB attenuation.

A stationary front lying a few miles north and west of the NSSL network sagged southward during the late morning, however, providing sufficient low-level convergence to set off weak convective storms over the northwest portion of the observing facility by midday. Events at low levels were simultaneously enhanced by daytime heating and the passage of a strongly diffluent upper short-wave trough during the early afternoon hours. As a result a few moderate thunderstorms developed between 1200 and 1500 CST, one of which is the subject of this study.

Figure 1a shows the PPI radar configuration of the storm specimen towards the end of its mature stage and figures 1b and 1c are coincident RHI profiles recorded by the NSSL MPS-4 and RFF airborne RDR 1-D radars. The first echo appeared on the NSSL WSR-57 shortly after 1400 CST, and evolution through maturity and complete dissipation had occurred by 1630 CST. Radar reflectivity at maximum intensity approached  $10^5 \text{ mm}^6 \text{ m}^{-3}$  for short intervals between 1500 and 1530 CST, and during this period the echo height consistently exceeded 45,000 ft above ground. Dissipation proceeded slowly from 1540 through 1620 CST as the echo top receded at an average rate of about  $2 \text{ m sec}^{-1}$ .

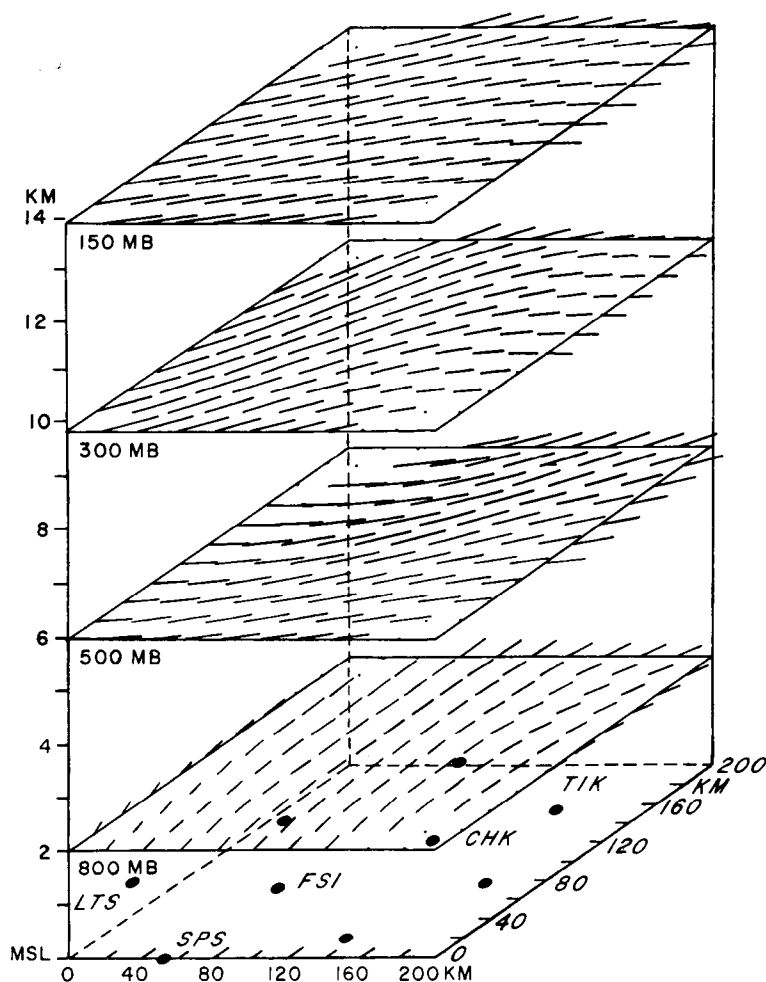


Figure 2. Three-dimensional representation of horizontal wind at 1530 CST, May 28, 1967, over south-central Oklahoma; interpolated from serial rawinsonde observations obtained at locations designated as dots ( $10 \text{ m sec}^{-1} = 20 \text{ km}$ ).



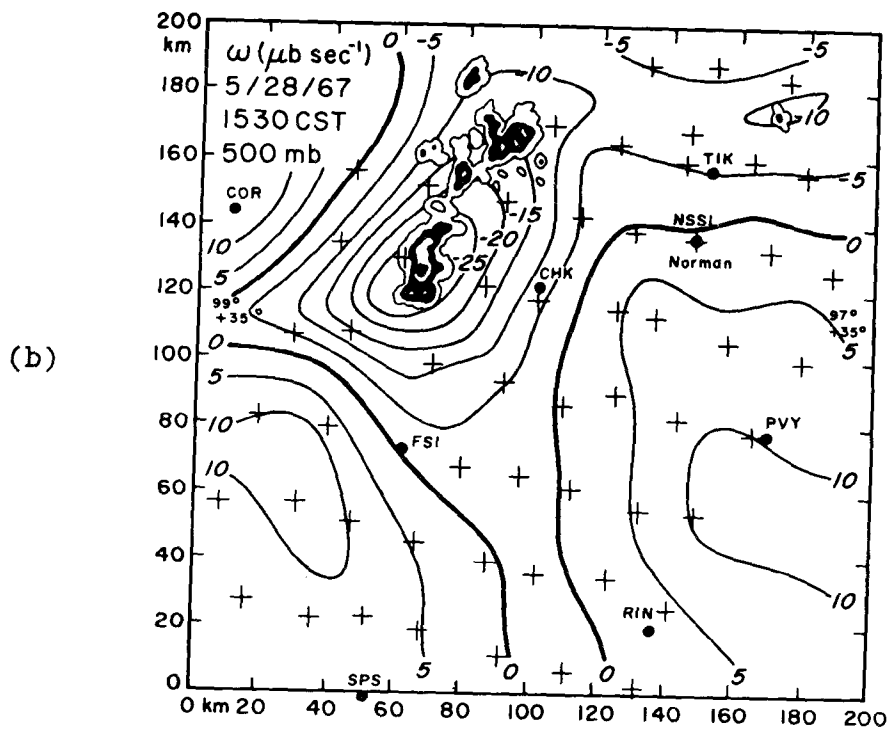
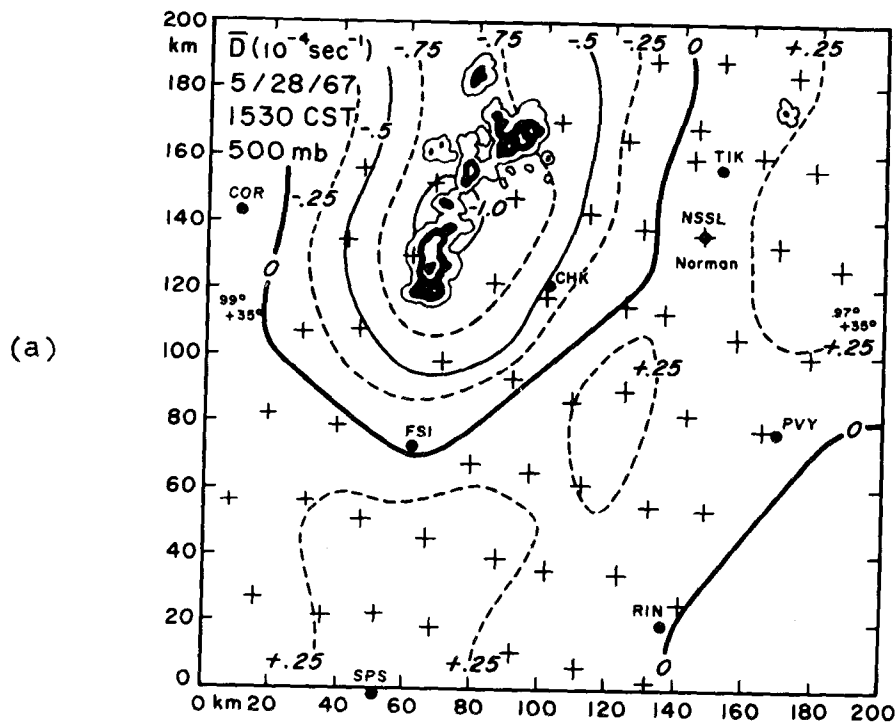


Figure 3. PPI radar echo configuration at 1530 CST, May 28, 1967.  
 (a) Divergence of horizontal wind (units,  $10^{-4} \text{ sec}^{-1}$ ).  
 (b) Vertical motion (units,  $\mu\text{b sec}^{-1}$ ) at 500 mb ( $1 \mu\text{b sec}^{-1} \approx -1.5 \text{ cm sec}^{-1}$ ).

Echo velocity ( $247^\circ/8 \text{ m sec}^{-1}$ ) was remarkably constant throughout the lifetime of the storm. Direction of travel was about  $20^\circ$  to the right of, and  $1 \text{ m sec}^{-1}$  less than, the mean wind in the troposphere ( $225^\circ/9 \text{ m sec}^{-1}$ ).

A special network of nine rawinsonde stations obtained soundings to 100 mb at 90-min intervals between 1100 and 1700 CST, within a 240-by-240-km area surrounding the other NSSL facilities. Computer programs developed to produce synoptic portrayal of the sounding data allow for balloon drift from the point of release and take account of nonsimultaneous releases.

Figure 2 is a three-dimensional representation of the horizontal wind at 1530 CST interpolated from the serial soundings. Divergence of the horizontal wind at 500 mb is presented in figure 3a, and the associated vertical motion field derived from the equation of continuity is shown in figure 3b. Precipitation echo intensity contours from the NSSL WSR-57 radar are superimposed on both fields.

### 3. EXPERIMENTAL AND ANALYTICAL PROCEDURES

A meteorologically instrumented DC-6, operated by the ESSA Research Flight Facility, systematically sounded the cloud's environment throughout its mature and dissipating stages. Two clockwise circumnavigations flown at the 500-mb level between 1500 and 1550 CST were followed by three more at the 800-mb level during the period 1600 to 1630 CST. Aircraft tracks and winds measured by the Doppler navigational system, positioned relative to the radar echo center, are displayed in figures 4a and 4b.

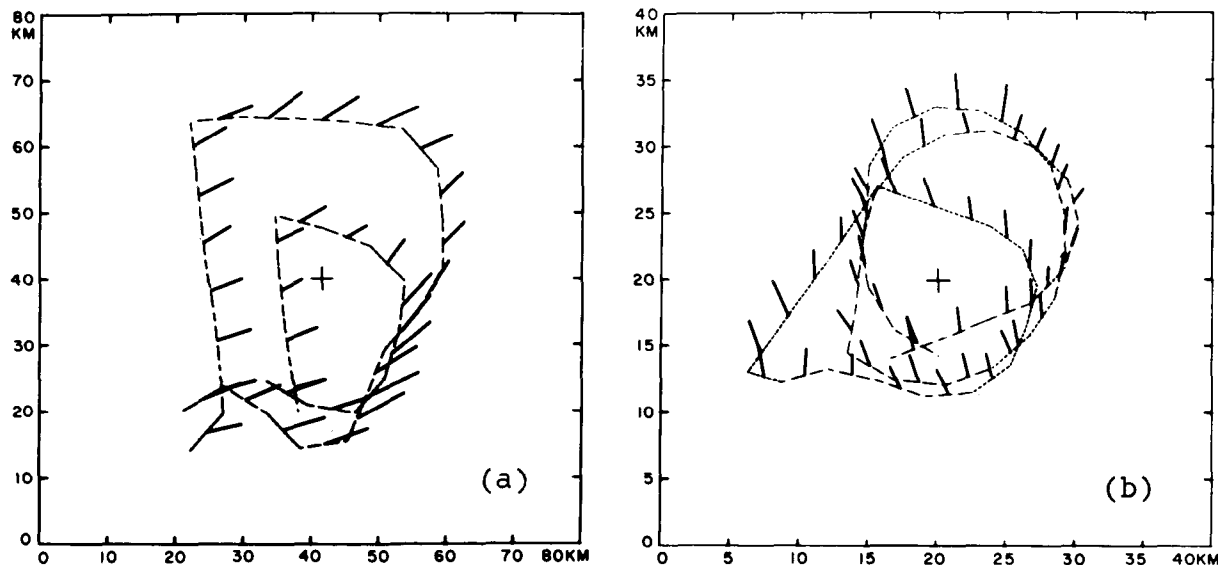


Figure 4. (a) Aircraft track and winds at 500 mb, averaged over 1 min and positioned relative to radar echo centered at cross. Outer loop flown between 1503 and 1530 CST; inner circuit, 1534-1551 CST ( $10 \text{ m sec}^{-1} = 5 \text{ km}$ ). (b) Same as (a) except data collected between 1559 and 1634 CST at 800 mb and averaged over 30-sec intervals ( $10 \text{ m sec}^{-1} = 2.5 \text{ km}$ ).

Seven chaff packets were ejected from the aircraft at 500 mb on the northward-bound upwind leg of the outer loop, and a few minutes later six more were released in the downwind cloud region (see fig. 5). A deposition interval of 45 sec and average airspeed of  $110 \text{ m sec}^{-1}$  resulted in a space separation of approximately 5 km between targets.

Individual chaff dipoles consisted of metallic-coated Fiberglas needles, with diameters of 0.0075 inch ( $\approx 190\mu$ ) cut at the wavelength of the L band tracking radar. Manufacturer specifications indicate a radar cross section of  $80 \text{ cm}^2$  and a terminal velocity of  $0.5 \text{ ft sec}^{-1}$  ( $\approx 15 \text{ cm sec}^{-1}$ ).

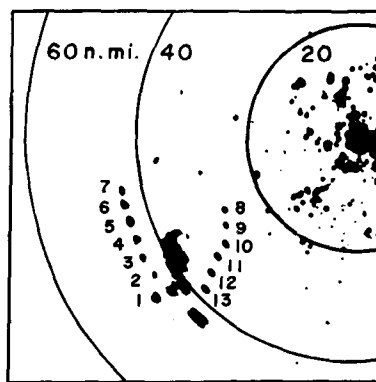


Figure 5. OKC, FAA, ARSR-1D, MTI, PPI at 1527 CST. Chaff targets numbered according to order of deposition. Research aircraft IFF appears south of storm echo.

Magnitudes of the mesoscale vertical air motions shown in figure 3b indicate that the chaff's net motion in the vertical could range from nearly zero to  $\pm 1 \text{ km hr}^{-1}$ . In response to average winds of  $15 \text{ m sec}^{-1}$ , horizontal displacement amounted to  $54 \text{ km hr}^{-1}$ , or more than 50 times the largest vertical displacement that might be expected. Lateral displacement of the chaff can, therefore, be taken as a reasonably accurate definition of the horizontal wind at the altitude of release.

Chaff position was recorded by time-lapse photography of the PPI scope of an ARSR-1D navigational control radar located at the Oklahoma City-Will Rogers Airport, an FAA facility. The radar, operated in MTI mode throughout the tracking experiment, accepted only those targets that had a radial velocity larger than a threshold set in the design of the equipment (usually  $1$  to  $2 \text{ m sec}^{-1}$ ). Radar returns coming from targets having lower radial speeds were therefore strongly attenuated. The possible effect of this on analytical interpretation is discussed later.

Soon after the chaff was released from the aircraft, individual echoes had an appearance characteristic of point targets, in that beam-width effects resulted in stretching normal to the beam axis, as shown in figure 5. With time, however, further elongation takes place, and orientation shifts so that the echo's major axes no longer intersect radar radials at right angles. The situation is schematically portrayed in figure 6.

Lateral expansion of the chaff target with time is undoubtedly a result of eddy diffusion, while heterogeneous terminal fall velocities combined with the effects of vertical shear account for the eventual

$\Delta S$  ; ECHO DISPLACEMENT

( )<sub>L</sub> ; LEFT EDGE

( )<sub>R</sub> ; RIGHT EDGE

$$\bar{V} = \Delta S / (t_2 - t_1)$$

$$\bar{V}_S = \bar{V}_L - \bar{V}_R$$

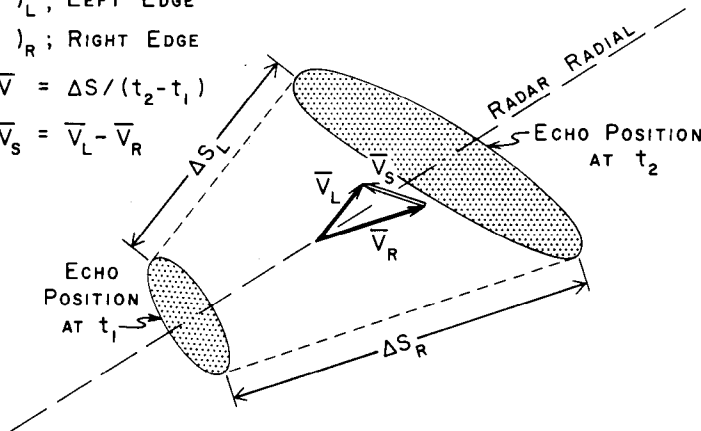


Figure 6. Schematic representation of chaff echo displacement and lateral spread.

skewedness with respect to the beam axis. Wexler (1951) proposed similar conditions in explaining the spread of volcanic debris following the Krakatoa eruption.

Considering the normal condition of veering wind with height, it is likely that those chaff elements forming the right forward part of the overall target undergo the least vertical displacement with time and best approximate the wind at the level of emission into air flow. Conversely, the left rear section of the chaff echo is apt to consist of needles that have experienced the greatest downward motion. A tendency for needles to cluster would undoubtedly affect the chaff's response characteristics and thereby provide a mechanism contributing to differential terminal fall velocities. Note also that the difference between winds derived from the displacements of the opposite ends of the chaff echo represents the shear of the horizontal wind in the layer through which chaff with maximum terminal velocity has fallen.

Proximity balloon soundings and aircraft winds measured during descent from 500 to 800 mb showed that both the upstream and downstream winds veered with heights; therefore, following the above reasoning, the extreme right forward edge of individual targets was used to evaluate chaff displacement. Upwind targets could be tracked with great accuracy for up to an hour, while downwind elements, although deposited later, deteriorated as identifiable entities much more quickly. Upstream, the chaff distribution was normal to the ambient airflow, and the elements could be clearly distinguished and reliably positioned. Downstream, however, an unfortunate choice of aircraft heading resulted in deposition along the flow and made displacement continuity difficult to establish. Furthermore, upstream components parallel to the radar radials were large, while downstream target motion, from a more southerly direction, resulted in occasional echo cancellation (for reasons discussed earlier), because the packets had only small components along

the radar beam axis. As indicated in the next section, difficulty in analyzing downstream chaff might also be attributed to a more turbulent airflow in the wake region of the cloud.

In the analysis, chaff positions were evaluated at 5-min intervals. With assumed total response to the airflow, trajectories and associated winds were derived by smoothing displacement increments over 10-min intervals. Upwind chaff trajectories are shown with the storm's displacement in figure 7a. Streamlines relative to the cloud at 1545 CST were derived by subtracting storm motion from chaff displacement. These appear in figure 7b.

#### 4. DISCUSSION OF RELATIVE AIRFLOW

Figure 8b is an interpretation of the relative air motion surrounding the cloud at the 500 mb level, derived from the vector field shown in figure 8a. Solid vectors represent chaff winds, and the superimposed dashed arrows are coincident aircraft measurements averaged over 1-min intervals. The chaff and aircraft data positioned closely in time and space generally agree within 1 or 2 m sec<sup>-1</sup>.

If the circulation is, to some degree, nonstationary, the winds measured during the first and largest circuit should agree best with earliest, upwind chaff vectors, and apparently do. Interior loop winds recorded between 1535 and 1550 CST depart considerably from both chaff and outer loop winds, possibly, as indicated by RHI profiles, because

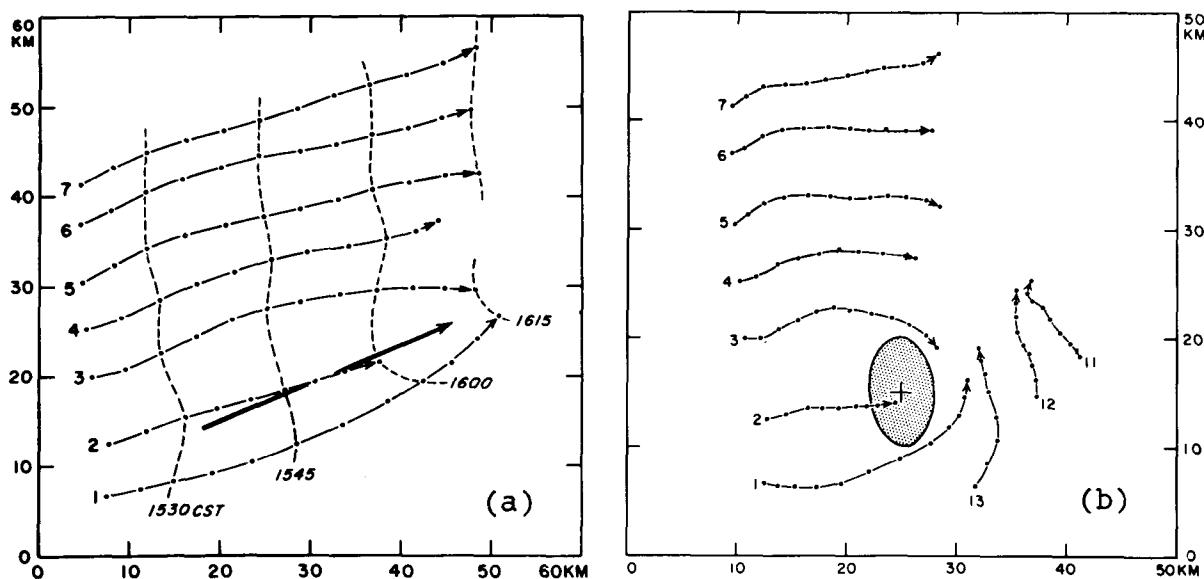


Figure 7. (a) Trajectories of chaff targets 1 through 7, shown in fig. 4. Bold vector represents storm translation between 1515 and 1615 CST. (b) Relative streamlines derived by subtracting storm motion from chaff displacement. Note that streamline 2 crosses echo boundary defined by NSSL, WSR-57, PPI.

the precipitation echo was changing from a quasisteady state to the dissipating stage during the same period.

The derived flow pattern in figure 8b is similar in many respects to the circulation recorded by Prandtl (1934) around a rotating cylinder embedded in a uniform water stream (fig. 9). In general, it also agrees with that described by Fujita and Grandoso (1966) for an isolated cumulonimbus that developed in a considerably stronger wind regime. Chaff winds are clearly diffluent immediately upwind, while winds from both data sources demonstrate a tendency for confluence in the downwind, wake region. Relative velocity, which averages about  $5 \text{ m sec}^{-1}$  in the undisturbed air stream, accelerates to maxima of  $10 \text{ m sec}^{-1}$  on the storm's right flank and  $7$  to  $8 \text{ m sec}^{-1}$  on the echo's left side. There is a deficit flow of  $1$  to  $2 \text{ m sec}^{-1}$  over a broad portion of the downstream vector field that reflects the resistance imposed by the storm on the uniform flow.

Although the streamlines in figure 8b suggest essentially laminar flow, the early dissipation of the three downwind chaff elements numbered 8, 9, and 10 in figure 5 suggests a wake flow that may be quite turbulent in character. Because it was difficult to establish displacement continuity, the analysis for these targets initially lying

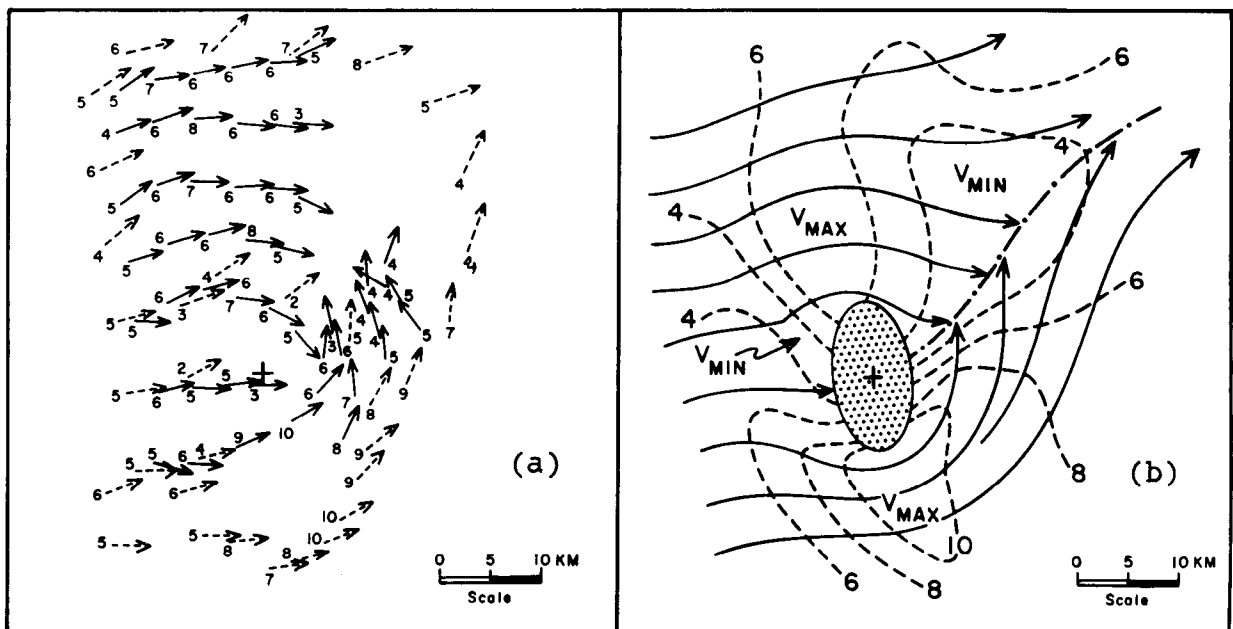


Figure 8. (a) Composite relative wind field with respect to storm echo centered on cross, derived from aircraft measurements (dashed) and chaff displacement (solid). Vector magnitude ( $\text{m sec}^{-1}$ ) appears at tail. (b) Simplified streamline and isoch pattern relating to data in (a). Dash-dot line denotes wake axis.

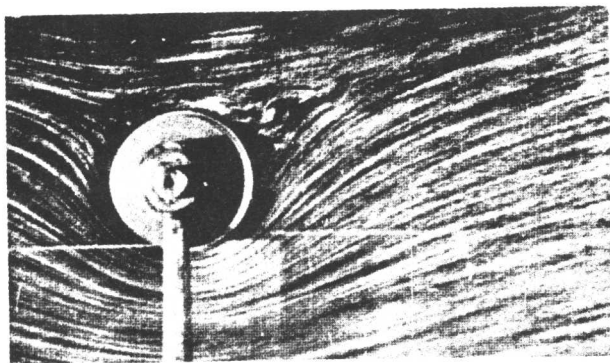


Figure 9. Flow about a stationary cyclonically rotating cylinder embedded in uniform water stream moving from left to right. Ratio of tangential velocity at cylinder periphery to speed of uniform flow is 3 (after Prandtl and Tietjens, 1934, fig. 14, plate 8).

closest to the wake axis was somewhat ambiguous. This ambiguity, attributed in part to the MTI radar technique, may have been compounded by irregular displacement and rapid target diffusion caused by eddies of a scale smaller than the analysis resolution.

Highest wind speed located in the field of maximum cyclonic curvature implies the existence of net cyclonic relative vorticity. Relative circulation, computed from aircraft wind components tangent to the circuit enclosing the storm, is on the order of  $18 \times 10^4 \text{ m}^2 \text{ sec}^{-1}$ . This value, divided by the area encompassed by the aircraft track ( $\approx 10^3 \text{ km}^2$ ), results in a relative vorticity of  $2 \times 10^{-4} \text{ sec}^{-1}$ .

An average tangential velocity,  $v_t$ , of  $1.5 \text{ m sec}^{-1}$  is estimated at the circuit boundary by taking the ratio of circulation and track length. As suggested previously by the author (Fankhauser, 1967), if absolute circulation,  $\Gamma_a$ , is conserved in moving from the track to the radar echo boundary,  $v_t$  near the storm's periphery can be estimated from  $v_t = (\Gamma_a - fA)/2\pi r$ , where  $f$  denotes Coriolis parameter,  $A$  the area of the radar echo, and  $r$  its mean radius. Using the value of the relative circulation already given,  $\Gamma_a$  becomes  $26 \times 10^4 \text{ m}^2 \text{ sec}^{-1}$ . Taking  $r = 5 \text{ km}$ , and  $A = 78 \times 10^6 \text{ m}^2$  from the storm's PPI configuration, substitution in the above equation yields  $8 \text{ m sec}^{-1}$  for  $v_t$  at the echo boundary.

Barnes (1968) used the vorticity equation and the shear in the low-level winds observed in this case to evaluate the contribution of the "tilting term" in the production of vorticity in the subcloud layer. He calculated that in 30 min its influence alone could generate vorticity of order  $2.7 \times 10^{-3} \text{ sec}^{-1}$ . This estimate does not include the effect of vertical stretching (the "divergence term"), which would conceivably increase the magnitude in the storm's updraft. In all likelihood, therefore, the tangential speeds near the echo boundary were even greater than  $8 \text{ m sec}^{-1}$ , estimated on the basis of potential flow in the environment at mid-cloud levels.

A horizontal lift force analogous to the hydrodynamical "Magnus effect" is directly proportional to both the tangential velocity,  $v_t$ , at the obstacle boundary and the speed of the undisturbed stream,  $v_o$ .

At the same time, Prandtl's experimental results show that the coefficient of lift is dependent on the ratio,  $v_t/v_o$ . In their discussion of possible steering forces that might be exerted on an obstructive rotating cloud, Fujita and Grandoso (1966) point out that lift forces are not likely to be effective until the rotational speed approaches the relative wind speed. From data similar to those dealt with here, they obtain an estimate of  $v_t/v_o = 1.5$ . This may be compared with the 1.6 derived from the data discussed here and to the 3 associated with Prandtl's laboratory experiment shown in figure 9.

Recall that the storm's motion vector was oriented  $20^\circ$  to the right of the mean flow in the troposphere and that its speed was on the order of  $1 \text{ m sec}^{-1}$  less than that of the mean wind. Newton's and Fankhauser's (1964) empirical formula, relating storm size to deviations from mean wind, indicates that an echo of the diameter observed here should move statistically nearly along the mean flow. Qualitatively, therefore, it appears that forces owing to drag that evolve from the storm's obstructive and rotational properties play a significant role in determining its motion.

The history of one of the upstream chaff targets, on the other hand, demonstrates quite clearly that internal draft circulations are not totally insulated from the external flow. While upstream targets, labeled 1 and 3 in figure 7b, diverge and accelerate relative to the storm, element 2 eventually becomes absorbed by the precipitation echo. Horizontal divergence at flight level, evaluated by integrating wind components normal to the closed aircraft track, amounts to  $-3 \times 10^{-4} \text{ sec}^{-1}$ , while analysis in figure 3a indicates convergence of order  $-1 \times 10^{-4} \text{ sec}^{-1}$  in the general area of the thunderstorm. Thus, independent data sources substantiate net convergence at the level of chaff deposition, which is consistent with the observed entrainment of the chaff target.

The entrained chaff element attains zero relative velocity when it is located to the right and rear of the echo center. Although the region of cloud entry is probably influenced by the target's original position with respect to the storm, the path of this particular element agrees with Browning's (1964) analysis of midlevel air trajectories. Considering relative motions based on typical severe storm velocities and vertical shear profiles, he surmised that the most efficient ingress of potentially cool air should take place on the cloud's right rear flank.

A wet-bulb temperature,  $\theta_w$ , of  $23^\circ\text{C}$  was characteristic of air overlying the surface surrounding the storm. As determined from surface network data recorded beneath the radar echo,  $\theta_w$  reached a minimum value of  $20^\circ\text{C}$  during the period of highest rainfall rate. Aircraft temperature and moisture measurements at 500 mb, both upstream and downstream, indicate  $\theta_w$  values of  $18.5^\circ\text{C}$ ; and nearby rawinsonde soundings reveal that the potentially coolest air existed near 600 mb where values ranged as low as  $17^\circ\text{C}$ .



Since mixing within the storm tends to equalize temperatures, the comparison of  $\theta_w$  in the ambient air aloft with those at the surface beneath and surrounding the storm, combined with the echo's observed ingestion of chaff, seems to substantiate what has long been considered a necessary condition for explaining the energy budget of persistent cumulonimbi: the air participating in the downdraft circulation enters the cloud at an intermediate level aloft.

## 5. SUMMARY AND CONCLUSIONS

The analyses presented in this memorandum serve to further establish the premise that mature thunderstorms act as effective barriers to air currents in the middle troposphere, and the observed merger of chaff and precipitation echoes supports the proposition that ambient air is simultaneously drawn into thunderstorm circulations at intermediate levels aloft. To quote from Hirschfeld (1960): "A storm is neither a rigid structure which is acted on en bloc by the winds, nor is it an amorphous mass, every part of which yields separately to the wind force exerted on it. It is rather a bit of each."

Although the qualitative nature of the relative flow around thunderstorms displays many features common to those observed in laboratory experiments, the extent to which classical hydrodynamics can be applied to storm and environment interactions will remain largely a matter of speculation until appropriate turbulence regimes and such relevant effects as viscosity are better defined. Particular caution should be exercised in the treatment of rotational aspects. As Dryden (1956) points out, the theoretical development relating to flow about rotating cylinders assumes a preexisting, nonvanishing circulation in the fluid and makes no provision for specifying its origin. From laboratory experiments it is clear that the circulation derives from the viscous interaction between the fluid and cylinder, but the assumption that this circulation is equal to the product of peripheral speed and circumference is not justified. Thus, there can be no adequate comparison between theory and experiment unless the circulation at the draft boundaries is actually measured. This is not likely to be done with conventional meteorological instrumentation, but some hope for defining air motion at the desired scales is provided by recent developments in the area of pulse-Doppler radar technology (Lhermitte, 1968).

The demonstrated utility of chaff as an air motion tracer appears to deserve further exploitation in thunderstorm research. Judicious deposition at various altitudes should make it possible to better define the differential airflow associated with thunderstorms and their surroundings. Such repeated experiments should obviously be supported by comprehensive radar coverage and independent wind measurements.